

Dual Modality Prompt Tuning for Vision-Language Pre-Trained Model

Yinghui Xing*, Qirui Wu*, De Cheng, Shizhou Zhang, Guoqiang Liang, Peng Wang, Yanning Zhang.

Abstract—With the emergence of large pre-trained vision-language model like CLIP, transferable representations can be adapted to a wide range of downstream tasks via prompt tuning. Prompt tuning tries to probe the beneficial information for downstream tasks from the general knowledge stored in the pre-trained model. A recently proposed method named Context Optimization (CoOp) introduces a set of learnable vectors as text prompt from the language side. However, tuning the text prompt alone can only adjust the synthesized “classifier”, while the computed visual features of the image encoder can not be affected, thus leading to sub-optimal solutions. In this paper, we propose a novel Dual-modality Prompt Tuning (DPT) paradigm through learning text and visual prompts simultaneously. To make the final image feature concentrate more on the target visual concept, a Class-Aware Visual Prompt Tuning (CAVPT) scheme is further proposed in our DPT, where the class-aware visual prompt is generated dynamically by performing the cross attention between text prompts features and image patch token embeddings to encode both the downstream task-related information and visual instance information. Extensive experimental results on 11 datasets demonstrate the effectiveness and generalization ability of the proposed method. Our code is available in <https://github.com/fanrena/DPT>.

Index Terms—Few-shot learning, Transfer learning, Image Classification, Prompt Tuning, Vision-Language Model

I. INTRODUCTION

Recently, researches in large-scale Vision-Language Models (VLM), such as CLIP [1] and ALIGN [2], have achieved remarkable progress in representation learning [3]–[5]. Benefiting from huge amounts of image-text data, the pre-trained large-scale vision-language model is able to learn open-set visual concept generated from natural language, thus further allows zero-shot transfer to downstream tasks. Specifically, the vision-language model is composed of two components: the image encoder and the text encoder. When a new classification task arrives, one can synthesize the classifier by feeding the natural language description of the classes to the text encoder. And then compute similarity between the “classifier” and the image features generated by the image encoder.

However, adapting these pre-trained large scale vision-language models efficiently to downstream tasks demonstrates its own challenge. Recent studies show that “prompting” is a simple and effective way [1], while designing a proper prompt is a non-trivial task. It always requires many domain

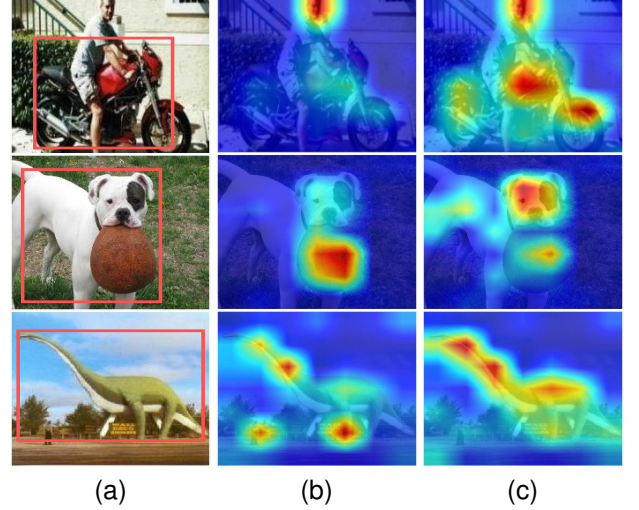


Fig. 1. Visualization of the attention map of the image encoder. (a) Original Image. (b) Zero-Shot CLIP/CoOp. (c) Our DPT. The images are selected from OxfordPets, and Caltech101. The GT annotated object is marked by a red box. Best viewed in color.

expertise and takes significant amount of time for manually words tuning. Usually even with massive tuning, we could not yet guarantee that the obtained prompt is optimal for the downstream tasks.

Recent researches on prompt learning for vision representation are mainly inspired by some prompt tuning approaches in Natural Language Processing (NLP) [6]–[8], e.g., the representative CoOp [9]. These methods proposed to model learnable contexts in prompt using continuous representations, and then trained the model with these learnable prompts in an end-to-end way while keeping the pre-trained parameters fixed. Although these methods have achieved great success and show promising performance at present, they only learn prompts for the text encoder.

From the perspective of conventional visual recognition, a typical vision model can be roughly divided into a feature extraction module and a classifier. Similarly, the process of feeding the text prompt into the text encoder can be viewed as the synthesis of a classifier, and the image encoder extracts the visual features. Assume that the large scale pre-trained vision-language models have already captured most of the general knowledge (visual concepts) for the downstream tasks. What the prompting mechanism actually do is to query the suitable information, which is beneficial to the downstream tasks, from the pre-trained model. As shown in Figure 1, for an input image with multiple visual objects (concepts), e.g.,

Yinghui Xing, Qirui Wu, Shizhou Zhang, Guoqiang Liang, Peng Wang, Yanning Zhang are with School of Computer Science, Northwestern Polytechnical University, Xi’an, China. De Cheng is with School of Telecommunications Engineering, Xidian University, Xi’an, China. Corresponding author is De Cheng (email: dcheng@xidian.edu.cn)

*The first two authors equally contributed to this work.

the first case contains a person and a motorbike, and the image encoder will extract all the visual features of the objects, i.e., the attention maps of Zero-Shot CLIP and CoOp highlight on both the person and motorbike. However, the downstream task requires the output class label to be “motorbike”—the ground-truth annotation. CoOp actually tries to enable the model to output “motorbike” by adjusting the “classifier” alone, while keeping the given highlighted “person” and “motorbike” visual features unchanged. There is a consensus in vision community that—features matter [10]! Therefore, we believe that adopting prompt tuning for the text encoder alone while directly utilizing the fixed image encoder for the downstream task is sub-optimal. In this paper, we introduce the visual prompts in the image input space, and propose a Dual-modality Prompt Tuning (DPT) paradigm through learning text prompts and visual prompts for both the text and image encoder simultaneously, aiming at adapting the pre-trained model to downstream tasks via adjusting both the “classifier” and “visual features”.

Specifically, for the visual prompt tuning in a ViT based image encoder, we introduce only a small amount of trainable parameters in the input of the transformer blocks while keeping the pre-trained image encoder fixed. Inserting visual prompts can directly adjust the image patch token embeddings, i.e. image features, through the self-attention weights and absorbing the prompts-derived value vectors. To make the pre-trained model better transfer to the downstream task, we further introduce a Class-Aware Visual Prompt Tuning (CAVPT) mechanism into our DPT framework to help the final obtained image feature concentrate more on the target visual concept. Aiming at encoding both the task-related information and visual instance information into the visual prompts, the class-aware visual prompt is dynamically generated by performing the cross attention between text prompts features and visual image patch token embeddings. Finally, the proposed overall DPT paradigm is learned with text prompts, visual prompts, and class-aware visual prompts simultaneously. As shown in Figure 1, it greatly demonstrates that tuning the pre-trained models with our DPT shows more focused task-aware visual attention area.

The main contributions of this paper can be summarized from the following three aspects:

- The proposed method demonstrates a new Dual-modality Prompt Tuning paradigm for tuning the large pre-trained vision-language model, by simultaneously learning the visual and text prompts from both ends of text and image encoder.
- To encourage the visual prompts to explicitly contain downstream task-related information, we further introduce the class-aware visual prompt into our DPT, which is dynamically generated by performing cross attention between text prompts features and visual token embeddings.
- Extensive experimental results on 11 datasets demonstrate the effectiveness of the proposed method, and show superiority to other prompt-tuning approaches by a large margin, as well as the generalization ability.

The remainder of this paper is organized as follows. Section II introduces the related works. Details of our proposed method are elaborated in Section III. In Section IV, we conduct comprehensive experiments on 11 datasets used in prompt tuning, which demonstrates the effectiveness of our method. Finally, the conclusion of our work is presented in Section V.

II. RELATED WORK

A. Vision-Language Pre-trained Models

Learning visual representations under the supervision of natural language has been demonstrated to be effective and attracting lots of attention [1], [2], [11], [12]. For vision-language models, the image-text matching and the cross-modal contrastive learning are two important issues. In CLIP [1], two encoders related to the vision and language modalities are designed, and these image and text embeddings are then aligned using a symmetric cross entropy loss. Similarly, ALIGN [2] also utilizes a dual-encoder architecture, but it projects the image and text embeddings to the same semantic space to calculate the similarity scores between vision and language modalities, which makes the vision-language interaction more efficient. Both of them are pre-trained on a large-scale image-text datasets with the contrastive loss, and can be transferred to downstream task. Researches on transferring CLIP to various downstream tasks, such as image classification [9], [13]–[15], video-text retrieval [16], tracking [17], and so on [18]–[21], thrives. In order to boost the performance of CLIP to downstream tasks, CLIP-Adapter [13] introduces feature adapters on either visual or language branch and fine-tunes them on the few-shot classification task. Zhang et al. [14] further proposed a Training-Free CLIP-Adapter (i.e., TIP-Adapter), which creates the weights by a key-value cache model constructed from the few-shot training set. With much less training, TIP-Adapter is more efficient than CLIP-Adapter. As an alternative framework to reduce the gap between objective forms of model pre-training and fine-tuning, prompt-based learning becomes a hot topic in both NLP and computer vision communities. However, the discrepancy between two different modalities brings the difficulties in tuning the prompt. Recently, Zhou *et al.* [9] proposed a context optimization (CoOp) strategy to automatically learn the optimal prompts, which greatly boosts the recognition accuracy. Our work also focuses on transferring the pre-trained vision-language model to downstream tasks through prompting.

B. Prompt Learning

Prompt learning originated from the community of NLP [6], [7], [22], and originally refers to the application of a fixed function to the input tokens, which provides an instruction about the task to the model. In computer vision community, prompt learning is explored in both the visual models [23]–[25] and the vision-language models [1], [9], [15], [18], [26], where visual prompt tuning (VPT) [23] achieved significant performance gains with only a small amount of additional parameters, i.e., prompts, in the input space. For vision-language models, CoOp [9] brings continuous prompt optimization

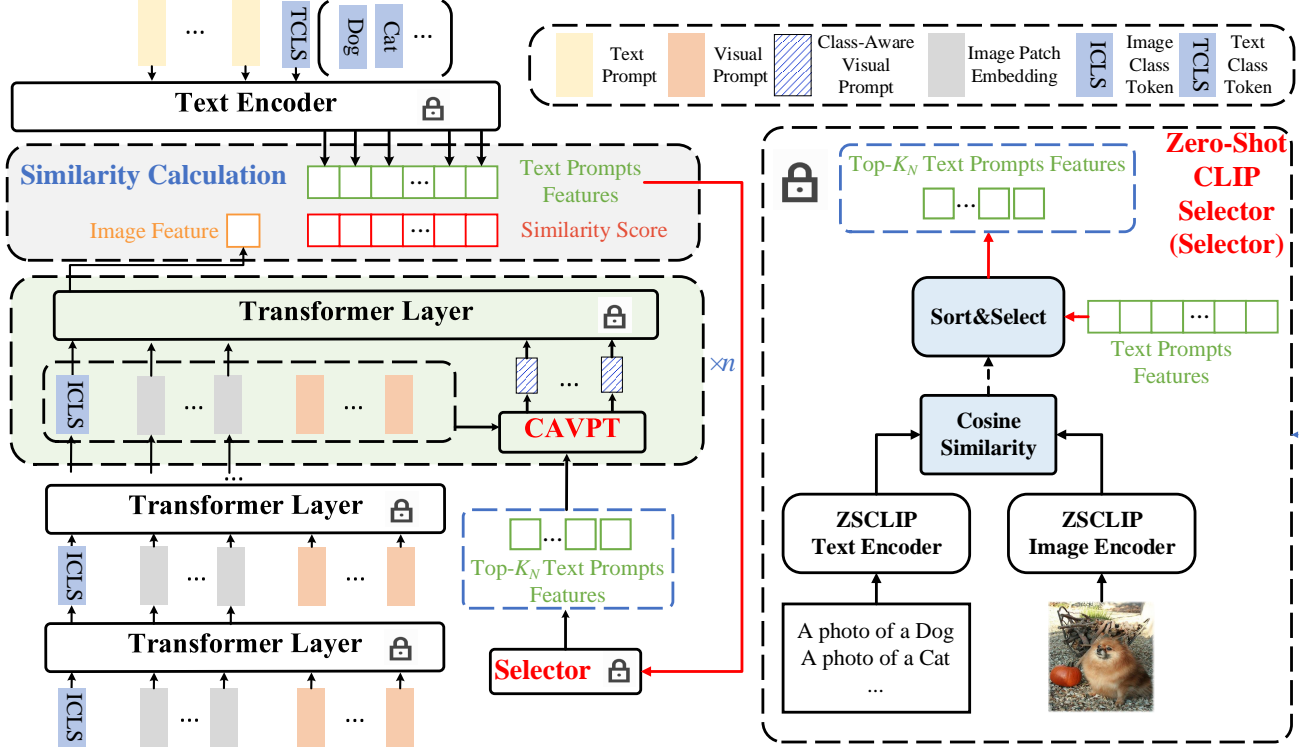


Fig. 2. The overall architecture of our proposed DPT method. It consists of three learnable components: text prompt, visual prompt and class-aware visual prompt generated from a Class-Aware Visual Prompt Tuning (CAVPT) module whose detailed architecture is illustrated in Figure 3.

from downstream data to adapt the pre-trained vision-language models. But CoOp may introduce improper prompt tuning steps which could hamper the general knowledge probing [26]. In order to improve the generalization ability of CLIP, Zhu *et al.* [26] proposed a novel prompt tuning method, *i.e.*, ProGrad, to deal with the conflicts between each tuning step and the general knowledge CLIP has predicted. Conditional CoOp (CoCoOp) [15] extends CoOp by learning an input-conditional token for each image to improve the cross domain generalization ability of CoOp. [27] learns the output embeddings of prompts instead of the input embeddings and employs a Gaussian distribution to model them effectively. [28] proposed a prompting method for CNN networks to adapt the pre-trained vision-language models to downstream tasks. [29] uses neural architecture search algorithm to identify the optimal configuration with adapters and prompts as small components. Most of the existing methods tune the prompts in the text encoders alone and neglect the clues in visual features. Our work proposes a Dual-modality Prompt Tuning paradigm, which introduces both the text prompt and visual prompt for vision-language model. Furthermore, class-aware visual prompt is proposed to enable the image feature to pay more attention to the target foreground object for downstream tasks.

C. Transfer Learning

Benefiting from the large scale of annotated data, the performance of deep neural networks has been greatly boosted. However, due to the labeling costs, collection of large scale training datasets with accurate annotations is cumbersome [14]. Trans-

fer learning [30]–[34], aiming to transfer general knowledge from one domain to some related domains with limited training data, has been proved to be a possible solution to few-shot learning [35]–[42]. Some works tried to tune a small amount of parameters while keeping most of the parameters of pre-trained models frozen. For example, [32] adapted the pre-trained network by training a lightweight side network that was fused with the frozen pre-trained network via summation. [33] proposed a new memory-efficient bias module, *i.e.* the lite residual module, to refine the feature extractor by learning small residual feature maps. While Rebuffi *et al.* [34] introduced an residual adapter to the model, and only trained the adapter network to improve the accuracy of domain-specific representations.

On the other hand, some self-supervised learning based methods, such as MoCo [43], BYOL [44], and MAE [45], can also alleviate the requirement of large-scale training data. Recently, vision-language models pre-trained on large-scale image-text pairs have demonstrated their superiority. Therefore, it is crucial to excavate the potentials of these models to downstream tasks. This paper focuses on transferring knowledges learned from them to downstream tasks through prompting.

III. METHODOLOGY

In this section, we first revisit CLIP model. Then we elaborate each component of the proposed Dual-modality Prompt Tuning (DPT) paradigm, including text prompt, visual prompt and class-aware visual prompt. Finally, we provide the loss function of DPT for training.

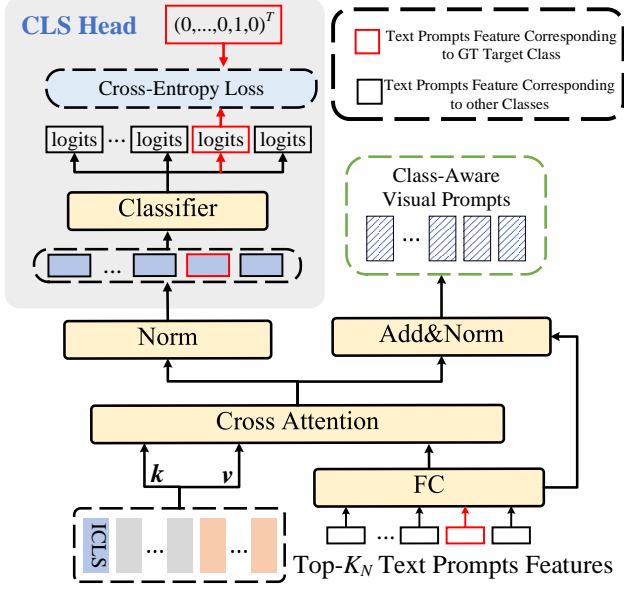


Fig. 3. The detailed architecture of the proposed Class-Aware Visual Prompt Tuning (CAVPT) module.

A. Contrastive Language-Image Pre-training (CLIP) Model

Contrastive language-image pre-training (CLIP) model aims to align image feature space and text feature space, which enables the model to have the capability of zero-shot transfer to downstream tasks. CLIP is composed of two encoders, one is designed for image and the other is for text. The text encoder adopts a transformer [46] to encode the text information while the image encoder can either be a CNN model, like ResNet [5], or be a vision transformer such as ViT [47]. In our method, we choose ViT as the image encoder for the compatibility of visual prompt in [23].

With a tremendous number of 400 million pairs of image-text samples, CLIP is trained under the contrastive learning framework, where the associated image and text are treated as positive samples, while the non-associated samples as negative samples. After that, the entire parameters of the pre-trained CLIP model are kept frozen to downstream tasks without any fine-tuning. In downstream tasks, a hand-crafted prompt is fed into the text end to synthesize a zero-shot linear classifier by embedding the class names of the target dataset. Taking the classification task as an example, “[CLASS]” token can be firstly extended by a template, such as “a photo of a [CLASS]”. Then the sentence is treated as a prompt and is encoded by the text encoder to derive a weight vector \mathbf{w}_i , $i = \{1, \dots, K\}$, where K is the total number of categories. At the same time, image features \mathbf{x} are obtained by the image encoder. The prediction probability can be calculated by

$$p(y = i | \mathbf{x}) = \frac{\exp(\text{sim}(\mathbf{x}, \mathbf{w}_i) / \tau)}{\sum_{j=1}^K \exp(\text{sim}(\mathbf{x}, \mathbf{w}_j) / \tau)}, \quad (1)$$

where $\text{sim}(\cdot, \cdot)$ represents the computation of cosine similarity, and τ is the temperature coefficient learned by CLIP.

B. Text Prompt and Visual Prompt

Text Prompt. It is known that hand-crafted prompt for CLIP model may take a lot of time and expertise for word tuning as a slight change in wording may lead to a significant performance degradation. Motivated by prompt tuning in NLP models, CoOp [9] introduces a set of tunable word embedding vectors to learn machine-favorable prompt for the text end which we call text prompt. Let $\{\mathbf{u}_1, \mathbf{u}_2, \dots, \mathbf{u}_M\}$ denote M learnable context vectors, and the word embedding of the text class token is represented by \mathbf{c}_i , $i = \{1, \dots, K\}$, then the prompt for the i_{th} class can be denoted as $\mathbf{t}_i = \{\mathbf{u}_1, \mathbf{u}_2, \dots, \mathbf{u}_M, \mathbf{c}_i\}$. By forwarding \mathbf{t}_i into the text encoder $g(\cdot)$, we can obtain a classification weight vector for the i_{th} visual concepts. The corresponding prediction probability can be calculated by,

$$p(y = i | \mathbf{x}) = \frac{\exp(\text{sim}(\mathbf{x}, g(\mathbf{t}_i)) / \tau)}{\sum_{j=1}^K \exp(\text{sim}(\mathbf{x}, g(\mathbf{t}_j)) / \tau)}, \quad (2)$$

where \mathbf{x} represents the extracted image features, and $g(\cdot)$ denotes the text encoder.

Visual Prompt. For vision-language models, there are two encoders for visual and language modalities. Tuning text prompt alone is not enough to reduce the gap between pre-trained and downstream tasks, thus leading to sub-optimal results. Motivated by the visual prompt tuning (VPT) [23] proposed for tuning vision transformers, we introduce visual prompt into the image encoder of CLIP model. The image patches $\{\mathbf{I}_j \in \mathbb{R}^{3 \times h \times w} | j \in \mathbb{N}, 1 \leq j \leq N_p\}$ are firstly embedded into a d -dimensional latent space as follows,

$$\mathbf{e}_0^j = \text{Embed}(\mathbf{I}_j) \quad \mathbf{e}_0^j \in \mathbb{R}^d, j = 1, 2, \dots, N_p. \quad (3)$$

Let $\mathbf{E}_l = \{\mathbf{e}_l^j \in \mathbb{R}^d | j \in \mathbb{N}, 1 \leq j \leq N_p\}$ and $\mathbf{P}_l = \{\mathbf{p}_l^i \in \mathbb{R}^d | i \in \mathbb{N}, 1 \leq i \leq P\}$ represent a collection of image patch embeddings and visual prompts for the l_{th} transformer layer, respectively. Suppose $\mathbf{s}_l \in \mathbb{R}^d$ is a learnable class token in image encoder, which is different from the text class token used in text prompt that the latter is a category-related word embedding. There are two versions of visual prompt, VPT-Shallow and VPT-Deep in [23]. We empirically found that VPT-Deep can achieve superior performances (See Table I), so we take VPT-Deep into our implementation in Section IV.

Visual prompts are introduced to each of the transformer layer, that is,

$$[\mathbf{s}_l, \dots, \mathbf{E}_l] = \Phi_l([\mathbf{s}_{l-1}, \mathbf{P}_{l-1}, \mathbf{E}_{l-1}]), l = 1, 2, \dots, L. \quad (4)$$

Generally, the performance is positively correlated with the prompt depth. Therefore, we utilize the VPT-Deep in our model. \mathbf{s}_L is then projected by a linear projection layer LP to obtain the final image feature. For simplicity, the whole process of image feature extraction can be represented by

$$\mathbf{x}' = f([\mathbf{s}_0, \mathbf{P}_0, \dots, \mathbf{P}_L, \mathbf{E}_0]), \quad (5)$$

where $f(\cdot)$ denotes the image encoder.

Note that the calculation process of the image encoder, i.e., the ViT model, can be viewed as a process of global scene reasoning and \mathbf{s}_l pools the visual concepts from the image patch embeddings layer-by-layer. With the help of visual prompts, the target visual concept corresponding to

TABLE I
MAIN RESULTS OF 11 DATASETS UNDER 16-SHOTS SETTING.

Methods	EuroSAT	Caltech101	Oxford Flowers	Food101	FGVC Aircraft	DTD	OxfordPets	Stanford Cars	Sun397	UCF101	ImageNet	Average
ZSCLIP [1]	45.49	91.28	66.63	80.62	19.08	44.03	87.38	60.19	62.06	63.52	59.61	61.81
CoOp [9]	83.12	94.45	95.07	78.20	33.94	67.20	88.88	75.79	72.31	79.10	66.55	75.87
CoCoOp [15]	74.99	94.01	79.97	82.36	23.64	59.34	<u>90.98</u>	64.25	69.75	73.13	65.07	70.68
ProGrad [26]	82.49	95.18	94.60	81.15	32.50	65.98	90.43	74.85	<u>73.22</u>	78.52	66.60	75.96
ProDA [27]	83.28	<u>95.5</u>	95.98	<u>81.89</u>	34.68	70.76	90.6	77.64	75.07	<u>81.85</u>	67.62	77.72
VPT	92.17	94.85	93.80	81.29	39.98	67.16	90.32	72.03	69.84	80.17	64.17	76.89
VLP	<u>91.90</u>	95.10	<u>96.05</u>	78.42	<u>42.92</u>	68.06	90.33	<u>78.81</u>	72.12	82.04	<u>66.91</u>	<u>78.42</u>
DPT	91.16	95.61	96.60	79.25	48.37	<u>70.16</u>	91.22	82.55	70.97	81.43	66.85	79.47

the downstream task may get more highlighted in \mathbf{s}_l via the self-attention operation in each transformer layer. By inserting visual prompts into each transformer layer, the self-attention operation for \mathbf{s}_l can be affected in two ways, as both the keys and values are actually get prepended through visual prompts: 1) The attention weights can be affected to allow \mathbf{s}_l to concentrate more on the image patch embeddings which includes target concept; 2) The visual prompts also serve as value vectors for the self-attention operation, so \mathbf{s}_l may absorb additional information that visual prompts learned.

However, the naïve visual prompts are devised as unconstrained learnable vectors, they can only learn some downstream task-related information implicitly by tuning the prompts on downstream task datasets. In this work, we propose Class-Aware Visual Prompt Tuning (CAVPT) to generate visual prompts by utilizing both the task-related information from the text side and instance-wise information from the visual side.

C. Class-Aware Visual Prompt Tuning

Class-aware visual prompts aims to explicitly encode task-related information. To this end, as shown in Figure. 2, for a downstream task with K classes, top- K_N text class token [CLASS] are firstly filtered out according to the zero-shot inference results for reducing the computational complexity. Then feeding the text prompts with the top- K_N text class token [CLASS] into the text encoder produces K_N feature vectors, i.e., $\mathbf{g}_j \in \mathbb{R}^D, 1 \leq j \leq K_N$, in which the task-related information are encoded. Class-aware visual prompt is generated dynamically by performing cross-attention between text prompts features from the text side and the inputs of the transformer block from the visual side.

After the mapping of a fully connected layer, we can get K_N query vectors $\mathbf{q}_j \in \mathbb{R}^d, 1 \leq j \leq K_N$. The key and value vectors $\mathbf{k} \in \mathbb{R}^{n \times d}$ are both obtained from the corresponding visual transformer layer’s inputs, including image patch embeddings, image class token embedding, and visual prompts. n stands for the total numbers of them. Our proposed class-aware visual prompt $\tilde{\mathbf{P}}_l^j \in \mathbb{R}^d$ for the l_{th} layer is computed as,

$$\mathbf{o}_l^j = \text{Softmax}\left(\frac{\mathbf{q}_j \mathbf{W}_q (\mathbf{k} \mathbf{W}_k)^T}{\sqrt{d_k}}\right) \mathbf{k} \mathbf{W}_v, 1 \leq j \leq K_N, \quad (6)$$

$$\tilde{\mathbf{P}}_l^j = LN(\mathbf{o}_l^j + \mathbf{q}_j), 1 \leq j \leq K_N, \quad (7)$$

where $LN(\cdot)$ denotes Layer Normalization. $\mathbf{W}_q \in \mathbb{R}^{d \times d_k}$, $\mathbf{W}_k \in \mathbb{R}^{d \times d_k}$, and $\mathbf{W}_v \in \mathbb{R}^{d \times d}$ denotes the parameters of cross attention.

To ensure the effect of the class-aware visual prompt, we additionally introduce a K -way classifier on top of the K_N outputs of the LN layer and cross entropy loss is enforced on the K -way logits as follows,

$$\mathcal{L}_{ce}^{ca} = - \sum_i \mathbf{y}_i \log p_i, 1 \leq i \leq K, \quad (8)$$

where p_i denotes the i_{th} logit from classifying $LN(\mathbf{o}_l^j)$, K denotes the number of classes and \mathbf{y} denotes the one-hot coding for the ground-truth target class. Note that only \mathbf{o}_l^j derived from \mathbf{q}_j which corresponds to the ground-truth target class will be classified.

As the image class token embedding in deeper layers usually contains more task-related semantic information, the class-aware visual prompt is only applied into the last few layers of the image encoder in our implementation.

D. Training of DPT

A Cross Entropy loss is adopted to minimize the distance between ground-truth annotation and the prediction probability computed by Equation (2).

$$\mathcal{L}_{ce} = - \sum_i \mathbf{y}_i \log p(y = i | \mathbf{x}''), 1 \leq i \leq K, \quad (9)$$

where \mathbf{y} denotes the ground-truth annotation, $p(y = i | \mathbf{x}'')$ denotes the predicted probability from Equation (2), and \mathbf{x}'' is the final obtained image feature,

$$\mathbf{x}'' = f([\mathbf{s}_0, \mathbf{P}_0, \dots, \mathbf{P}_l, \tilde{\mathbf{P}}_{l+1}^j, \dots, \tilde{\mathbf{P}}_L^j, \mathbf{E}_0]), \quad (10)$$

The total loss function combines the two cross entropy losses with a balancing hyper-parameter α as follows,

$$\mathcal{L}_{total} = \alpha \mathcal{L}_{ce}^{ca} + \mathcal{L}_{ce}. \quad (11)$$

For our proposed method VLP and DPT, we adopt a general knowledge guided warmup strategy in the first few epochs of training. Considering that CLIP model has stored the general knowledge, we train our model to learn from Zeroshot CLIP. The loss function we used for the first few epochs can be described as follows,

$$\mathcal{L} = \mathcal{L}_{coop} + \mathcal{L}_{vpt} + \beta \mathcal{L}_{ce} + \alpha \mathcal{L}_{ce}^{ca} \quad (12)$$

where \mathcal{L}_{coop} is the loss function we used for CoOp training, \mathcal{L}_{vpt} is the loss function we used in VPT training, and \mathcal{L}_{ce} is the loss function we used in VLP training. β is a balancing hyper-parameter. By changing loss function \mathcal{L}_{ce} in the first few epochs of VLP training to Equation (12), we use the general knowledge to guide the warmup process. During training, the proposed DPT keeps the entire parameters of both the image and text encoder fixed, while optimizing the Text prompt, Visual prompt and the parameters for generating class-aware visual prompt.

IV. EXPERIMENTS

A. Datasets and Implementation Details.

To evaluate the effectiveness of our method, we conduct experiments on 11 classification datasets, namely EuroSAT [48], Caltech101 [49], OxfordFlowers [50], Food101 [51], FGV-CAircraft [52], DTD [53], OxfordPets [54], StanfordCars [55], ImageNet1K [56], Sun397 [57], and UCF101 [58] as in [1, 9]. These datasets cover a wide range of computer vision tasks, including image classification on generic objects, fine-grained categories, satellite, texture, scene understanding and action recognition images.

Following the commonly used few-shot evaluation protocols as that in CLIP [1], we also adopt 1, 2, 4, 8, 16 shots for model training, and test it on the full test dataset. The reported results are averaged over three runs for fair comparison.

We adopt ViT-Base/32 as our backbone network for all experiments. All experiments are conducted based on CoOp [9] and CLIP [1] official released code. For VPT, the prompt length is set to 10 for each layer of the network, they are initialized the same way as text prompts in CoOp [9]. During model training, we adopt the SGD optimization method, the learning rate is decayed by the cosine rule. The maximum epoch for VPT is the same as CoOp [9]. Warming up trick is adopted during the first 10 epochs with a fixed learning rate of 10^{-5} on VPT. Learning rate for VPT is first searched in $\{0.01, 0.001, 0.0001, 0.00001\}$ and kept unchanged for visual prompts in all experiments. For the text prompts, we followed CoOp [9] with a context length of 16.

For our proposed method VLP and DPT, the maximum epoch is set to 100 for 16/8/4/2 shots, 60 epoch for 1 shot (The maximum epoch is set to 20 for ImageNet.) except for Caltech101 and OxfordPets in DPT, which is set to 60 for 16 shots scenario. Warming up trick is the same as in CoOp and VPT (The warmup epoch is set to 1 for ImageNet on both end). K_N is set to 10. And CAVPT is inserted into the last layer of the image encoder.

The balancing α is set to 0.3, β is set to 0.1. For the early training of VLP and DPT, the general knowledge is utilized as a guidance for the first 30 epochs (10 for ImageNet).

B. Comparison with Existing Methods

Existing representative prompt tuning methods include the remarkable CoOp method [9], and the CLIP model [1] itself used for zero-shot classification (i.e. Zero-Shot Clip). Therefore, we adopt these two models as our mainly compared methods.

Since our DPT additionally introduces visual prompts and class-aware visual prompts compared with text prompts alone in CoOp, to reveal how each ingredient contributes to the performance improvements, we additionally implement **VPT** and **VLP** besides **DPT** as follows,

- **VPT** standards for introducing naive visual prompt alone into the visual end of CLIP model [1] and hand-crafted text prompts, e.g. “a photo of a [CLASS]”, are adopted for the text end.

- **VLP** denotes the dual modality prompt tuning paradigm to simultaneously learn visual (V) and text (L) prompts, where the text prompt is designed the same as that in CoOp [9], and the visual prompt is exactly the same as VPT-Deep in VPT [23].

- **DPT** represents that we further integrate CAVPT into image encoder based on VLP.

The overall evaluation results are shown in Figure 4, which reports the classification accuracy on 11 datasets under all few-shots settings. Compared with the baseline methods, our DPT achieves superior performances on average over the 11 datasets. It can be clearly seen from Figure 4 and Table I that, 1) DPT greatly outperforms CoOp and Zero-shot CLIP by large margins. And the performance increases are basically proportional with the number of shots. Specifically, DPT outperforms Zero-shot CLIP by 17.6% and outperforms CoOp by 3.53% on average over the 11 datasets under the 16-shots settings. The results verified the superiority of the proposed DPT paradigm. 2) Comparing the results of VPT with CoOp, VPT gets better results than CoOp on average. Under the 16-shots setting, VPT can get 1% performance gains on average over all the 11 datasets. It shows that tuning the visual prompts from the image end instead of text prompts can get more effective results. It is worth noting that VPT and CoOp get inconsistent results on different datasets which indicates that tuning visual prompt and text prompt may have complementary effects. 3) Comparing the results of VLP than VPT and CoOp, VLP achieves better results than VPT and CoOp, which shows that tuning the dual modality prompts from both the visual and text ends is obviously better than tuning any single modality prompts for downstream task. 4) With the help of class-aware visual prompts, the results of our DPT can clearly be improved than VLP. Specifically, DPT gets 1% performance gains than VLP on average over 11 datasets under 16-shots setting, which shows the great significance of our CAVPT.

C. Domain Generalization

In this section, we aim to unveil how robust our method is to distribution shifts, in comparison to baseline methods.

Datasets. Following the setting in CoOp [9], we use ImageNet as the source dataset. And the target datasets are ImageNetV2 [59], ImageNet-Sketch [60], ImageNet-A [61], and ImageNet-R [62].

Setting. We choose CoOp and VPT as our baseline methods. All three method will be trained on the source dataset with 1 example per class and conduct zero-shot inference on target datasets.

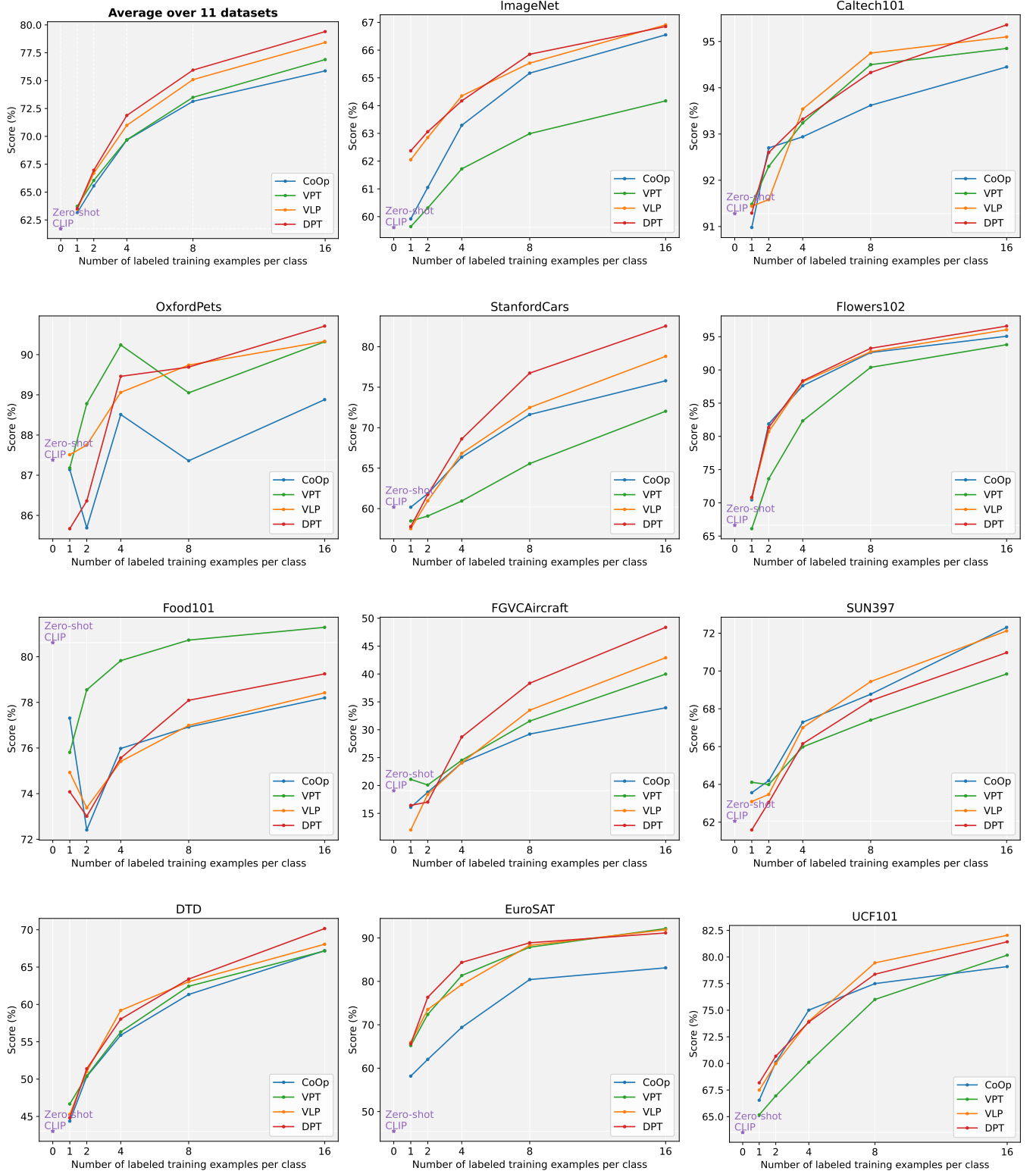


Fig. 4. Main results on the 11 datasets with 1,2,4,8,16 shots.

Results. As shown in Table III, Our method can achieve best performances on ImageNet, ImageNetV2, ImageNet-Sketch, ImageNet-R, while our method is less effective on ImageNet-

A which contains natural adversarial examples. This suggests that our method has stronger robustness than baseline methods but tends to be more vulnerable when facing adversarial

TABLE II
RESULTS OF 11 DATASETS UNDER 16-SHOTS SETTING WITH ViT-B/16.

Methods	EuroSAT	Caltech101	Oxford Flowers	Food101	FGVC Aircraft	DTD	OxfordPets	Stanford Cars	Sun397	UCF101	ImageNet	Average
ZSCLIP	47.69	93.75	70.69	<u>85.97</u>	24.81	43.09	89.07	65.55	62.61	67.54	64.51	65.03
CoOp	83.74	95.17	96.73	84.17	44.06	69.60	92.07	82.73	74.54	82.59	71.62	79.73
VPT	92.67	96.27	96.59	87.03	51.11	71.26	92.76	81.44	72.93	85.19	69.98	81.57
VLP	91.87	96.08	97.37	84.57	52.99	72.20	93.11	85.62	74.48	86.36	72.46	82.46
DPT	<u>92.10</u>	96.06	97.59	85.00	57.85	72.65	93.45	88.24	74.29	<u>85.31</u>	72.49	83.18

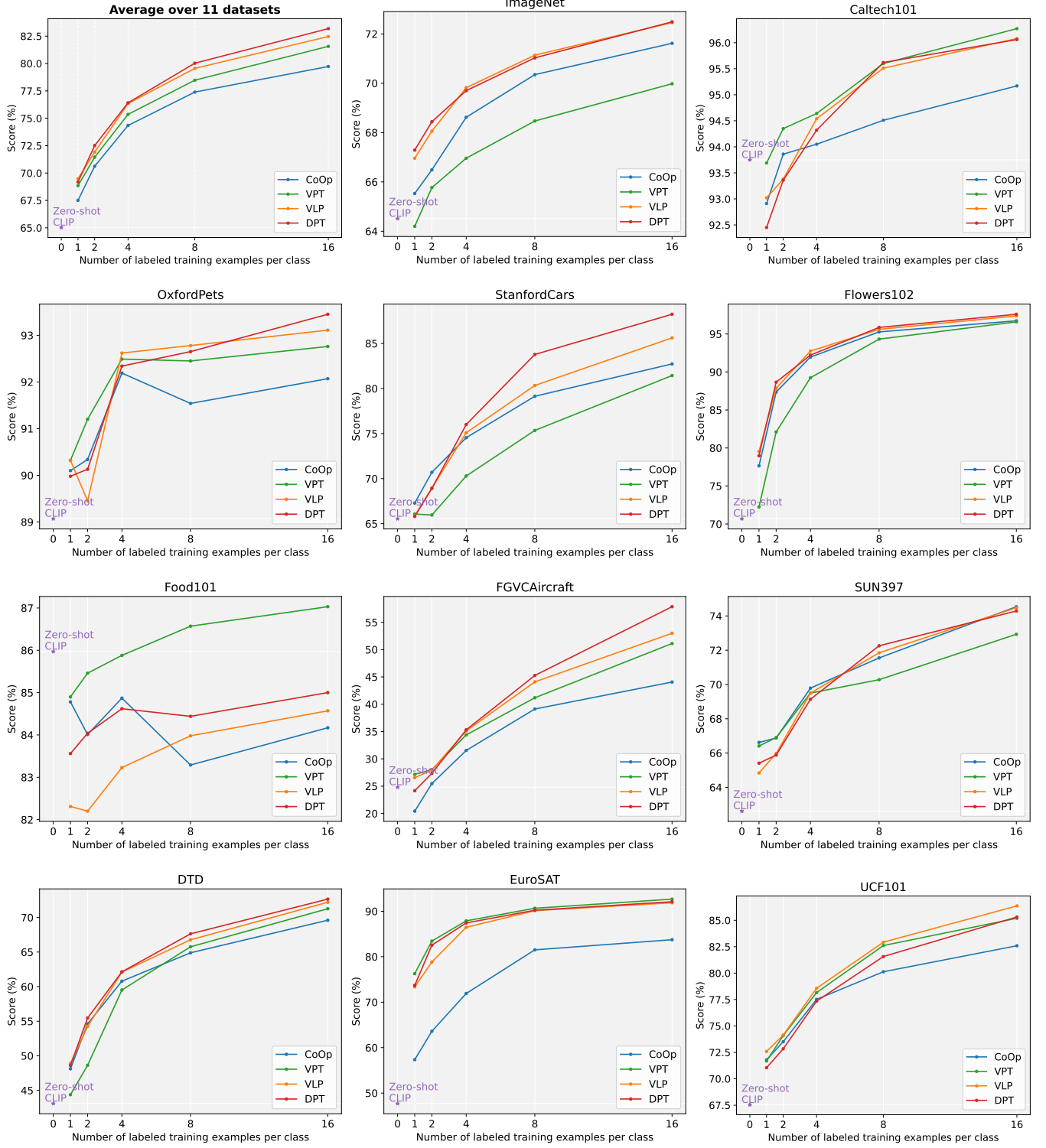


Fig. 5. Main results on the 11 datasets with 1,2,4,8,16 shots with ViT-B/16.

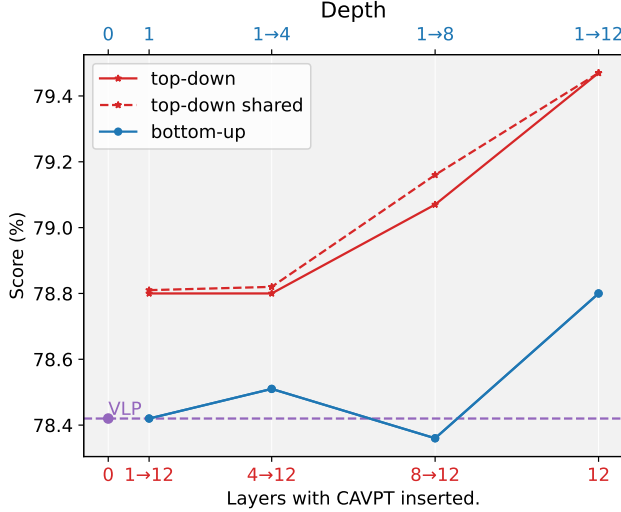


Fig. 6. The average accuracy on 11 datasets with different layers CAVPT inserted. $i \rightarrow j$ indicates the Transformer layer indice that CAVPT are inserted into.

examples compared with CoOp. In contrast, the VPT model obtains inferior results on target datasets, which shows that VPT is less robust compared with CoOp and our method.

D. Further Analysis

Analysis on the depth of CAVPT inserted into. CAVPT is a plug-and-play module and can be used in arbitrary layers of ViT backbone. In order to investigate the most suitable layers for CAVPT, we conduct comprehensive experiments in both bottom-up and top-down fashions with varying values of Depth, *i.e.* $\{1 \rightarrow 12, 4 \rightarrow 12, 8 \rightarrow 12, 12\}$ for top-down fashion and $\{1, 1 \rightarrow 4, 1 \rightarrow 8, 1 \rightarrow 12\}$ for bottom-up fashion, on top of the VLP model, on all 11 datasets. An extra experimental setting of sharing CAVPT across different layers are also conducted in the top-down fashion by sharing parameters of CAVPT. As shown in Figure 6, the results of the top-down fashion is much better than bottom-up fashion and the last layer of Transformer is the most suitable layer for CAVPT, suggesting that CAVPT would play a more important role at deeper layers. Additionally, comparing the shared CAVPT and vanilla CAVPT, the shared CAVPT can achieve a little better results while having fewer parameters.

Analysis on the length of CAVPT. To investigate the suitable length of CAVPT, we conduct comprehensive experiments on different length of CAVPT, *i.e.* $\{0, 1, 5, 10, 20, 50, 100\}$. 0 length indicates that the method deteriorates to VLP but without visual prompts in the last layer of ViT backbone. For some datasets, taking EuroSAT [48] as an example, it only contains 10 classes which is insufficient to obtain more than 10 CAVPT. Thus when the number of required CAVPT is larger than classes, we take the number of classes as the length of CAVPT to obtain the corresponding results. As shown in Table V, when setting the length to be 10, it achieves best accuracy.

Analysis of the loss function on CAVPT module. In the proposed CAVPT module, we apply the cross-entropy loss to

encourage the visual class token and the text prompts features to be aligned. In order to demonstrate the effectiveness of the loss function, we optimize the model with different α on the CAVPT module. The experimental results are shown in Table IV. We can clearly see that setting $\alpha = 0.3$ helps to improve the average accuracy by 0.44%, which significantly illustrates the efficacy of such a loss function.

Analysis of parameters of different model. Since DPT introduces more parameters than VLP and VPT, can VLP or VPT achieve same performance as DPT with the same amount of parameters? We increase the number of visual prompts to 120 for VLP and VPT to compare its performance with DPT under a competitive amount of parameters. Note that CoOp limits the input token number. Thus CoOp are not discussed in this section. As shown in Table VI, with larger number of visual prompts, both VPT and VLP’s performance dropped drastically, suggesting that simply enlarging the parameter size will hamper the performance.

TABLE III
COMPARISON WITH SINGLE MODAL PROMPT METHODS ON ROBUSTNESS TO DISTRIBUTION SHIFT UNDER 1-SHOT SCENARIO.

Method	ImageNet	-V2	-S	-A	-R	Average	OOD Average
CoOp [9]	59.92	52.88	37.32	28.52	62.12	48.15	45.21
VPT	59.64	52.18	35.74	21.31	59.93	45.76	42.29
DPT	62.37	55.15	39.65	27.79	64.79	49.95	46.85

TABLE IV
THE AVERAGE ACCURACY ON 11 DATASETS WITH DIFFERENT α .

α	0	0.1	0.3	0.5	0.7	1
Average	78.96	79.27	79.47	79.25	79.28	79.27

TABLE V
THE AVERAGE ACCURACY ON 11 DATASETS WITH VARIOUS LENGTHS OF CAVPT.

Length	0	1	5	10	20	50	100
Average	78.41	79.21	79.29	79.47	79.35	79.28	79.33

TABLE VI
DPT VS BIGGER VLP VS VPT ON 11 DATASETS UNDER 16 SHOTS SETTING. VCTX STANDS FOR THE NUMBER OF VISUAL PROMPTS.

Methods	# params	Average
VPT(VCTX=10)	92,160	76.89
VPT(VCTX=120)	1,105,920	73.64
VLP(VCTX=10)	100,352	78.42
VLP(VCTX=120)	1,114,112	71.71
DPT	1,136,384	79.47

Analysis of different backbone. To further show the effectiveness of our method, we conduct experiments on ViT-B/16 backbone. As shown in Fig 5 and Table II, DPT outperforms Zero-shot CLIP and CoOp by 18.15% and 3.45% on average over the 11 datasets under 16-shots settings, which

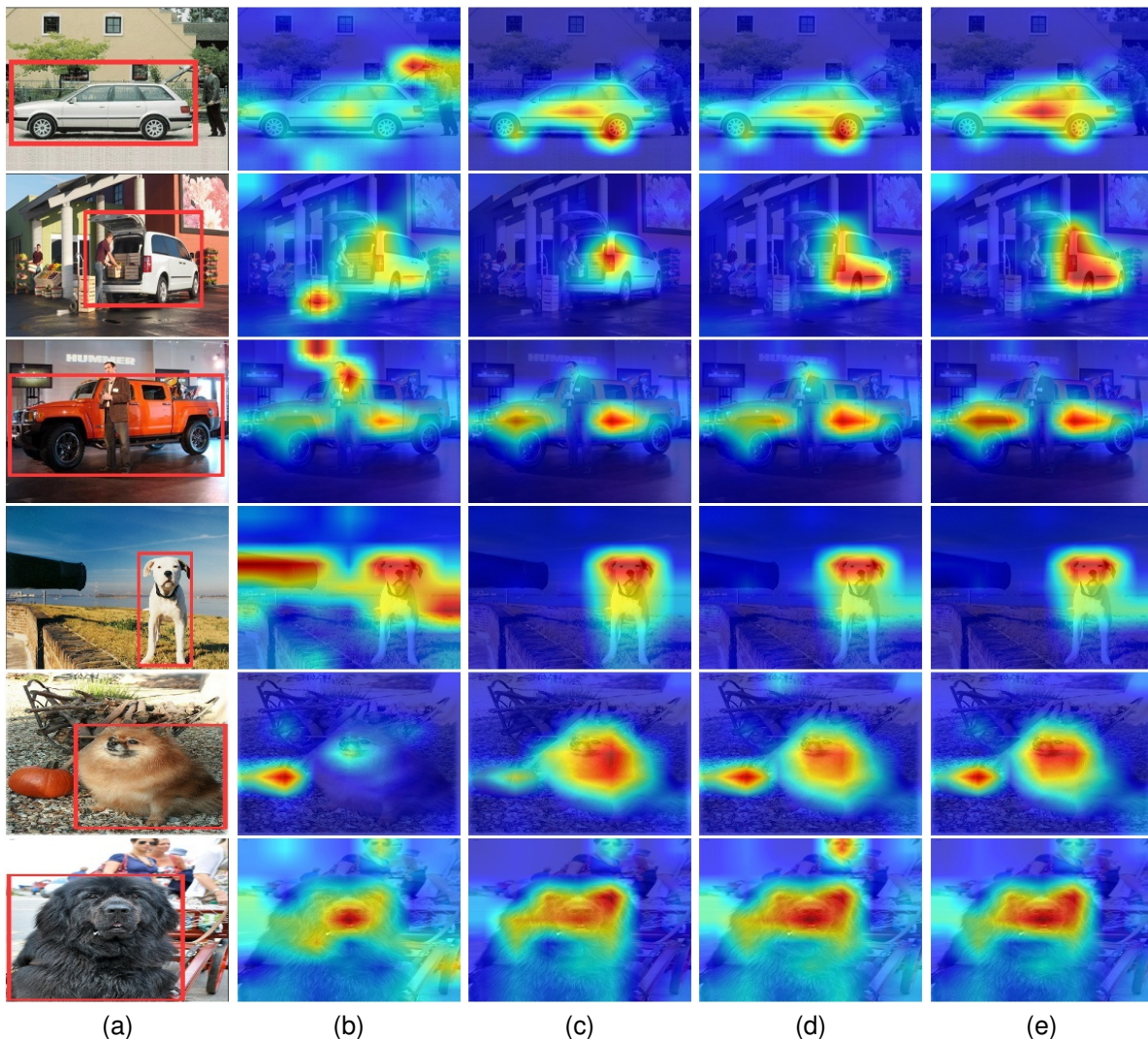


Fig. 7. Comparison of attention map visualization of the variant methods. (a) Original Image. (b) Zero-shot CLIP/CoOp. (c) VPT-Deep. (d) VLP. (e) DPT. The GT annotated object is marked by a red box.

demonstrates the superiority of DPT with other backbones. The same conclusions can also be drawn that tuning the visual prompts is more effective than text prompts, and the joint tuning of visual-text prompts also boosts the classification accuracy.

In summary, the experimental results under the ViT-B/16 backbone are consistent with that under ViT-B/32 backbone, which indicates the effectiveness and the reasonability of dual modality prompt tuning.

E. Visualization of the attention map.

In Figure 1, we visualize and compare the attention map for the last layer of CoOp and our DPT tuned model to understand the proposed method in-depth. Figure 1 (a) shows the original images with target objects in red bounding boxes. Figure 1 (b) shows the attention maps of the baseline method Zero-shot CLIP/CoOp. As CoOp does not tune the image encoder, the attention maps are the same with Zero-shot CLIP. Figure 1 (c) depicts the attention maps of our proposed DPT method. It

can be clearly seen that Zero-shot CLIP/CoOp usually focuses on most of the typical objects in the image, while DPT tends to concentrate more on the target visual object (concept).

We show extra examples of visualization in Fig 7. All of these examples are sampled from StanfordCars and OxfordPets. In Figure 7(a), we annotated the object of interest in red box. Figure 7(b) demonstrates the attention map of Zeroshot CLIP/CoOp. As CoOp has no modification on image features, the attention maps are the same with ZS CLIP. It can be clearly seen that multiple objects are highlighted while only a little attention the model pays on the objects of interest in downstream tasks. In Figure 7(c), which shows the visualization of VPT, the object of interest is well highlighted. It shows that VPT have learned some downstream task-related knowledge. The visualization of VLP and DPT are shown in Figure 7(d) and (e). Comparing Figure 7(d) and Figure 7(e), the object of interest would be more concentrated and more non-related objects are less highlighted in Figure 7(e). It shows that CAVPT can help model to pay more attention on the right

object rather than other task non-related objects.

V. CONCLUSION

In this paper, we propose a new Dual-modality Prompt Tuning paradigm for tuning the large pre-trained vision-language model to downstream tasks via learning the visual and text prompts simultaneously. To make the final obtained image feature concentrate more on the target visual concept, we further encode both the downstream task-related information and image instance information into the visual prompt and propose class-aware visual prompts, which are dynamically generated by performing cross attention between text prompts features and image token embeddings. Extensive experimental results on 11 datasets demonstrate the effectiveness of the proposed method, and show superiority to other prompt tuning approaches by a large margin.

REFERENCES

- [1] A. Radford, J. W. Kim, C. Hallacy, A. Ramesh, G. Goh, S. Agarwal, G. Sastry, A. Askell, P. Mishkin, J. Clark *et al.*, “Learning transferable visual models from natural language supervision,” in *International Conference on Machine Learning*. PMLR, 2021, pp. 8748–8763.
- [2] C. Jia, Y. Yang, Y. Xia, Y.-T. Chen, Z. Parekh, H. Pham, Q. Le, Y.-H. Sung, Z. Li, and T. Duerig, “Scaling up visual and vision-language representation learning with noisy text supervision,” in *International Conference on Machine Learning*. PMLR, 2021, pp. 4904–4916.
- [3] K. Desai and J. Johnson, “Virtex: Learning visual representations from textual annotations,” in *Proceedings of the IEEE/CVF conference on computer vision and pattern recognition*, 2021, pp. 11 162–11 173.
- [4] Y. Zhang, H. Jiang, Y. Miura, C. D. Manning, and C. P. Langlotz, “Contrastive learning of medical visual representations from paired images and text,” *arXiv preprint arXiv:2010.00747*, 2020.
- [5] K. He, X. Zhang, S. Ren, and J. Sun, “Deep residual learning for image recognition,” in *Proceedings of the IEEE conference on computer vision and pattern recognition*, 2016, pp. 770–778.
- [6] T. Shin, Y. Razeghi, R. L. Logan IV, E. Wallace, and S. Singh, “Auto-prompt: Eliciting knowledge from language models with automatically generated prompts,” in *Proceedings of the 2020 Conference on Empirical Methods in Natural Language Processing (EMNLP)*, 2020, pp. 4222–4235.
- [7] Z. Jiang, F. F. Xu, J. Araki, and G. Neubig, “How can we know what language models know?” *Transactions of the Association for Computational Linguistics*, vol. 8, pp. 423–438, 2020.
- [8] B. Lester, R. Al-Rfou, and N. Constant, “The power of scale for parameter-efficient prompt tuning,” *arXiv preprint arXiv:2104.08691*, 2021.
- [9] K. Zhou, J. Yang, C. C. Loy, and Z. Liu, “Learning to prompt for vision-language models,” *International Journal of Computer Vision*, pp. 1–12, 2022.
- [10] R. Girshick, J. Donahue, T. Darrell, and J. Malik, “Rich feature hierarchies for accurate object detection and semantic segmentation,” in *Proceedings of the IEEE conference on computer vision and pattern recognition*, 2014, pp. 580–587.
- [11] Y.-C. Chen, L. Li, L. Yu, A. El Kholy, F. Ahmed, Z. Gan, Y. Cheng, and J. Liu, “Uniter: Universal image-text representation learning,” in *European conference on computer vision*. Springer, 2020, pp. 104–120.
- [12] Y. Li, F. Liang, L. Zhao, Y. Cui, W. Ouyang, J. Shao, F. Yu, and J. Yan, “Supervision exists everywhere: A data efficient contrastive language-image pre-training paradigm,” *arXiv preprint arXiv:2110.05208*, 2021.
- [13] P. Gao, S. Geng, R. Zhang, T. Ma, R. Fang, Y. Zhang, H. Li, and Y. Qiao, “Clip-adapter: Better vision-language models with feature adapters,” *arXiv preprint arXiv:2110.04544*, 2021.
- [14] R. Zhang, R. Fang, P. Gao, W. Zhang, K. Li, J. Dai, Y. Qiao, and H. Li, “Tip-adapter: Training-free clip-adapter for better vision-language modeling,” *arXiv preprint arXiv:2111.03930*, 2021.
- [15] K. Zhou, J. Yang, C. C. Loy, and Z. Liu, “Conditional prompt learning for vision-language models,” in *Proceedings of the IEEE/CVF Conference on Computer Vision and Pattern Recognition*, 2022, pp. 16 816–16 825.
- [16] H. Fang, P. Xiong, L. Xu, and W. Luo, “Transferring image-clip to video-text retrieval via temporal relations,” *IEEE Transactions on Multimedia*, 2022.
- [17] J. Yang, Z. Li, F. Zheng, A. Leonardis, and J. Song, “Prompting for multi-modal tracking,” in *Proceedings of the 30th ACM International Conference on Multimedia*, 2022, pp. 3492–3500.
- [18] Y. Rao, W. Zhao, G. Chen, Y. Tang, Z. Zhu, G. Huang, J. Zhou, and J. Lu, “Denseclip: Language-guided dense prediction with context-aware prompting,” in *Proceedings of the IEEE/CVF Conference on Computer Vision and Pattern Recognition*, 2022, pp. 18 082–18 091.
- [19] R. Zhang, Z. Zeng, Z. Guo, and Y. Li, “Can language understand depth?” in *Proceedings of the 30th ACM International Conference on Multimedia*, 2022, pp. 6868–6874.
- [20] R. Mokady, A. Hertz, and A. H. Bermano, “Clipcap: Clip prefix for image captioning,” *arXiv preprint arXiv:2111.09734*, 2021.
- [21] R. Zhang, Z. Guo, W. Zhang, K. Li, X. Miao, B. Cui, Y. Qiao, P. Gao, and H. Li, “Pointclip: Point cloud understanding by clip,” in *Proceedings of the IEEE/CVF Conference on Computer Vision and Pattern Recognition*, 2022, pp. 8552–8562.
- [22] P. Liu, W. Yuan, J. Fu, Z. Jiang, H. Hayashi, and G. Neubig, “Pre-train, prompt, and predict: A systematic survey of prompting methods in natural language processing,” *arXiv preprint arXiv:2107.13586*, 2021.
- [23] M. Jia, L. Tang, B.-C. Chen, C. Cardie, S. Belongie, B. Hariharan, and S.-N. Lim, “Visual prompt tuning,” *arXiv preprint arXiv:2203.12119*, 2022.
- [24] Z. Wang, Z. Zhang, C.-Y. Lee, H. Zhang, R. Sun, X. Ren, G. Su, V. Perot, J. Dy, and T. Pfister, “Learning to prompt for continual learning,” in *Proceedings of the IEEE/CVF Conference on Computer Vision and Pattern Recognition*, 2022, pp. 139–149.
- [25] H. Bahng, A. Jahanian, S. Sankaranarayanan, and P. Isola, “Exploring visual prompts for adapting large-scale models,” *arXiv preprint arXiv:2203.17274*, 2022.
- [26] B. Zhu, Y. Niu, Y. Han, Y. Wu, and H. Zhang, “Prompt-aligned gradient for prompt tuning,” *arXiv preprint arXiv:2205.14865*, 2022.
- [27] Y. Lu, J. Liu, Y. Zhang, Y. Liu, and X. Tian, “Prompt distribution learning,” in *Proceedings of the IEEE/CVF Conference on Computer Vision and Pattern Recognition*, 2022, pp. 5206–5215.
- [28] H. Bahng, A. Jahanian, S. Sankaranarayanan, and P. Isola, “Exploring visual prompts for adapting large-scale models,” *arXiv preprint arXiv:2203.17274*, vol. 1, no. 3, p. 4, 2022.
- [29] Y. Zhang, K. Zhou, and Z. Liu, “Neural prompt search,” *arXiv preprint arXiv:2206.04673*, 2022.
- [30] Y. Lu, W. Wang, C. Yuan, X. Li, and Z. Lai, “Manifold transfer learning via discriminant regression analysis,” *IEEE Transactions on Multimedia*, vol. 23, pp. 2056–2070, 2020.
- [31] P. Jing, Y. Su, L. Nie, and H. Gu, “Predicting image memorability through adaptive transfer learning from external sources,” *IEEE Transactions on Multimedia*, vol. 19, no. 5, pp. 1050–1062, 2016.
- [32] J. O. Zhang, A. Sax, A. Zamir, L. Guibas, and J. Malik, “Side-tuning: a baseline for network adaptation via additive side networks,” in *Computer Vision—ECCV 2020: 16th European Conference, Glasgow, UK, August 23–28, 2020, Proceedings, Part III 16*. Springer, 2020, pp. 698–714.
- [33] H. Cai, C. Gan, L. Zhu, and S. Han, “Tinytl: Reduce memory, not parameters for efficient on-device learning,” *Advances in Neural Information Processing Systems*, vol. 33, pp. 11 285–11 297, 2020.
- [34] S.-A. Rebuffi, H. Bilen, and A. Vedaldi, “Learning multiple visual domains with residual adapters,” *Advances in neural information processing systems*, vol. 30, 2017.
- [35] Y. Zhu, W. Min, and S. Jiang, “Attribute-guided feature learning for few-shot image recognition,” *IEEE Transactions on Multimedia*, vol. 23, pp. 1200–1209, 2020.
- [36] H. Zhang, H. Li, and P. Koniusz, “Multi-level second-order few-shot learning,” *IEEE Transactions on Multimedia*, 2022.
- [37] H. Cheng, J. T. Zhou, W. P. Tay, and B. Wen, “Graph neural networks with triple attention for few-shot learning,” *IEEE Transactions on Multimedia*, 2023.
- [38] K. Guo, C. Shen, B. Hu, M. Hu, and X. Kui, “Rsnet: relation separation network for few-shot similar class recognition,” *IEEE Transactions on Multimedia*, 2022.
- [39] H. Huang, J. Zhang, J. Zhang, J. Xu, and Q. Wu, “Low-rank pairwise alignment bilinear network for few-shot fine-grained image classification,” *IEEE Transactions on Multimedia*, vol. 23, pp. 1666–1680, 2020.
- [40] P. Tian, H. Yu, and S. Xie, “An adversarial meta-training framework for cross-domain few-shot learning,” *IEEE Transactions on Multimedia*, 2022.

- [41] X. Zhong, C. Gu, M. Ye, W. Huang, and C.-W. Lin, "Graph complemented latent representation for few-shot image classification," *IEEE Transactions on Multimedia*, 2022.
- [42] L. Zhang, Y. Du, J. Shen, and X. Zhen, "Learning to learn with variational inference for cross-domain image classification," *IEEE Transactions on Multimedia*, 2022.
- [43] K. He, H. Fan, Y. Wu, S. Xie, and R. Girshick, "Momentum contrast for unsupervised visual representation learning," in *Proceedings of the IEEE/CVF conference on computer vision and pattern recognition*, 2020, pp. 9729–9738.
- [44] J.-B. Grill, F. Strub, F. Altché, C. Tallec, P. Richemond, E. Buchatskaya, C. Doersch, B. Avila Pires, Z. Guo, M. Gheshlaghi Azar *et al.*, "Bootstrap your own latent-a new approach to self-supervised learning," *Advances in neural information processing systems*, vol. 33, pp. 21 271–21 284, 2020.
- [45] K. He, X. Chen, S. Xie, Y. Li, P. Dollár, and R. Girshick, "Masked autoencoders are scalable vision learners," in *Proceedings of the IEEE/CVF Conference on Computer Vision and Pattern Recognition*, 2022, pp. 16 000–16 009.
- [46] A. Vaswani, N. Shazeer, N. Parmar, J. Uszkoreit, L. Jones, A. N. Gomez, L. Kaiser, and I. Polosukhin, "Attention is all you need," *Advances in neural information processing systems*, vol. 30, 2017.
- [47] A. Dosovitskiy, L. Beyer, A. Kolesnikov, D. Weissenborn, X. Zhai, T. Unterthiner, M. Dehghani, M. Minderer, G. Heigold, S. Gelly, J. Uszkoreit, and N. Houlsby, "An image is worth 16x16 words: Transformers for image recognition at scale," *ICLR*, 2021.
- [48] P. Helber, B. Bischke, A. Dengel, and D. Borth, "Eurosat: A novel dataset and deep learning benchmark for land use and land cover classification," *IEEE Journal of Selected Topics in Applied Earth Observations and Remote Sensing*, vol. 12, no. 7, pp. 2217–2226, 2019.
- [49] L. Fei-Fei, R. Fergus, and P. Perona, "Learning generative visual models from few training examples: An incremental bayesian approach tested on 101 object categories," in *2004 conference on computer vision and pattern recognition workshop*. IEEE, 2004, pp. 178–178.
- [50] M.-E. Nilsback and A. Zisserman, "Automated flower classification over a large number of classes," in *2008 Sixth Indian Conference on Computer Vision, Graphics & Image Processing*. IEEE, 2008, pp. 722–729.
- [51] L. Bossard, M. Guillaumin, and L. V. Gool, "Food-101—mining discriminative components with random forests," in *European conference on computer vision*. Springer, 2014, pp. 446–461.
- [52] S. Maji, E. Rahtu, J. Kannala, M. Blaschko, and A. Vedaldi, "Fine-grained visual classification of aircraft," *arXiv preprint arXiv:1306.5151*, 2013.
- [53] M. Cimpoi, S. Maji, I. Kokkinos, S. Mohamed, and A. Vedaldi, "Describing textures in the wild," in *Proceedings of the IEEE conference on computer vision and pattern recognition*, 2014, pp. 3606–3613.
- [54] O. M. Parkhi, A. Vedaldi, A. Zisserman, and C. Jawahar, "Cats and dogs," in *2012 IEEE conference on computer vision and pattern recognition*. IEEE, 2012, pp. 3498–3505.
- [55] J. Krause, M. Stark, J. Deng, and L. Fei-Fei, "3d object representations for fine-grained categorization," in *Proceedings of the IEEE international conference on computer vision workshops*, 2013, pp. 554–561.
- [56] J. Deng, W. Dong, R. Socher, L.-J. Li, K. Li, and L. Fei-Fei, "Imagenet: A large-scale hierarchical image database," in *2009 IEEE conference on computer vision and pattern recognition*. Ieee, 2009, pp. 248–255.
- [57] J. Xiao, J. Hays, K. A. Ehinger, A. Oliva, and A. Torralba, "Sun database: Large-scale scene recognition from abbey to zoo," in *2010 IEEE computer society conference on computer vision and pattern recognition*. IEEE, 2010, pp. 3485–3492.
- [58] K. Soomro, A. R. Zamir, and M. Shah, "Ucf101: A dataset of 101 human actions classes from videos in the wild," *arXiv preprint arXiv:1212.0402*, 2012.
- [59] B. Recht, R. Roelofs, L. Schmidt, and V. Shankar, "Do imagenet classifiers generalize to imagenet?" in *International Conference on Machine Learning*. PMLR, 2019, pp. 5389–5400.
- [60] H. Wang, S. Ge, Z. Lipton, and E. P. Xing, "Learning robust global representations by penalizing local predictive power," *Advances in Neural Information Processing Systems*, vol. 32, 2019.
- [61] D. Hendrycks, K. Zhao, S. Basart, J. Steinhardt, and D. Song, "Natural adversarial examples," in *Proceedings of the IEEE/CVF Conference on Computer Vision and Pattern Recognition*, 2021, pp. 15 262–15 271.
- [62] D. Hendrycks, S. Basart, N. Mu, S. Kadavath, F. Wang, E. Dorundo, R. Desai, T. Zhu, S. Parajuli, M. Guo *et al.*, "The many faces of robustness: A critical analysis of out-of-distribution generalization," in *Proceedings of the IEEE/CVF International Conference on Computer Vision*, 2021, pp. 8340–8349.